PROCEEDINGS, 48th Workshop on Geothermal Reservoir Engineering
Stanford University, Stanford, California, February 11-13, 2023
SGP-TR-214

A new modelling study of the Kamojang geothermal field

John O'Sullivan[1]*, Fathan Abdurachman[3], Greg Bignall[4], Chris Bromley, Ken Dekkers[1], Muhammad Ghassan[2], Michael Gravatt[1], Pudyo Hastuti[3], Astri Indra[2], Rony Nugraha[12], Fernando Pasaribu[3], Joris Popineau[1], Imam Prasetyo[3], Vicky Rai[2], Theo Renaud[1], Jeremy Riffault[1], Dhanie Yuniar[3], Michael O'Sullivan[1]

[1]Department of Engineering Science, University of Auckland, Private Bag 92019, Auckland, New Zealand

[2]Geoenergi Solusi Indonesia (Geoenergis), Cibis Nine 11th Floor, Jakarta, Indonesia

[3]PT. Pertamina Geothermal Energy, Jakarta, 10340, Indonesia

[4]G&A Geothermal Advice Limited, Taupo 3330, New Zealand

*jp.osullivan@auckland.ac.nz

Keywords: Kamojang, Geothermal reservoir simulation, Integrated modelling, AUTOUGH2, Waiwera

ABSTRACT

Indonesia has the second highest geothermal power installed capacity worldwide and expects to develop more geothermal energy in the future. Kamojang is a vapour-dominated geothermal field located 40 km to the southeast of Bandung in West Java, Indonesia. It was the first geothermal project to be developed in Indonesia.

In this paper we discuss a multidisciplinary approach to a new modelling study of the Kamojang Geothermal Field (KGF), Indonesia. The project team included members from PT. Pertamina Geothermal Energy, the Geothermal Institute at the University of Auckland, Geoenergis Solusi Indonesia, and independent New Zealand geothermal experts. It successfully achieved its objectives through close collaboration and an inclusive, transparent approach.

A review and update of the conceptual model of the KGF has been conducted. The updated conceptual model was set up as a digital conceptual model in the Leapfrog software and used to develop a new numerical model. In setting up the numerical model we use an integrated modelling framework developed at the University of Auckland that allows the direct creation of a numerical model from a Leapfrog-based digital conceptual model. The numerical model can be run in AUTOUGH2, a local variant of the industry-standard simulator TOUGH2, or in Waiwera, a highly parallelised, open-source simulator developed by the University of Auckland and GNS Science.

The new numerical model was calibrated against the measured data using the industry-standard approach. The state of model calibration achieved is good and we are confident that the model provides a good representation of the KGF and is appropriate to use for forecasting.

1. INTRODUCTION

Kamojang is a vapour-dominated geothermal field located 40 km to the southeast of Bandung in West Java, Indonesia. It was the first geothermal project to be developed in Indonesia. It is currently producing from 5 geothermal power plants (total installed capacity of 235 MW_e). A pilot plant began operation in 1978 and the first commercial power plant was commissioned in 1983. Over the years, 94 wells have been drilled: 58 production wells, 6 injection wells, 21 monitor wells and 9 wells have been abandoned.

In 2022 a collaborative project to study the KGF was initiated between PT. Pertamina Geothermal Energy (PGE), the Geothermal Institute at the University of Auckland (UoA), Geoenergis Solusi Indonesia (Geoenergis) and independent New Zealand geothermal experts. The objective of the project was to carry out a detailed resource assessment of the system using the most up-to-date data, analyses and numerical modelling techniques. There were several stages involved in the project:

1. Reviewing the updated field data
2. Updating the conceptual model
3. Updating the Leapfrog digital conceptual model
4. Reviewing the existing numerical model
5. Developing a new numerical modal
6. Calibrating the numerical model
7. Using model forecast to assess the future potential of the KGF

The multidisciplinary project team included geoscientists, engineers, analysts and managers from each of the organisations. The project successfully achieved its objectives through close collaboration and an inclusive, transparent approach. The updated conceptual model, the updated Leapfrog digital conceptual model and the new numerical model not only provided an appropriate framework for carrying out the resource assessment, but they also are invaluable tools for ongoing studies of the KGF. Details of the main stages in the project and the resulting models are discussed in the following sections.

2. CONCEPTUAL MODEL

2.1 Conceptual Model Update

All the available geoscientific and reservoir engineering data regarding Kamojang was reviewed by our multidisciplinary project team. The results of the collaborative review were that the updated conceptual model is broadly consistent with previous studies described by Prasetyo et al. (2020) and with past investigations of surface thermal manifestations, including early studies by New Zealand investigators (such as Wood, 1975; Browne, 1977; Healy, 1977; and Hochstein, 1975). Figure 1 shows a representative cross-section through the system by Prasetyo et al. (2020) and the updated conceptual model is summarised as follows.

Kamojang is centred on the WSW-ENE trending Quaternary Guntur-Rakutak volcanic complex in Central Java, an approximately 15 km-long chain of overlapping caldera and other volcanic centres. There are seven main lithological units, the eruptive products of G. Cibatuipis, G. Pangkalan, G. Gandapura, G. Kancing, G. Masigit, G. Gajah and G. Guntur. The volcanic activity is superimposed on a major regional, fault-controlled graben-like structure. The Kendang Fault is a tensional structure marking the NE-SW boundary of the graben to the west and the Pateungteung and Citepus Faults bound the eastern margin of the resource. The other prominent structure in the Kamojang area is the two-km wide Pangkalan Caldera. Faults provide secondary permeability in the KGF and are inferred to be associated with past volcano-tectonic events. These include the sub-circular collapse of Pangkalan in the central part of the KGF, the NE-SW trending fault network and the graben representing the most pronounced aspect of the NW-SE trending tensional fault system. The Kamojang heat source is inferred beneath Gandapura-Cakra and Pangkalan Caldera.

From the study of hydrothermal minerals in drillcore (and fluid inclusion data), the present-day vapour-dominated reservoir which characterises the KGF is inferred to have evolved from a previous hot water system through sealing/changes in pathways over geological time-scales. Surface geothermal manifestations occur in the NE part of the Kamojang area, adjacent to the Gandapura volcanic complex. The manifestations are predominantly steam-heated features and include steaming / altered ground, fumaroles, solfatara, hot acid-sulphate springs. The hydrothermal mineral assemblage includes silica (as cristobalite and quartz), rare replacement albite and vug-filling adularia and epidote. Calcite is abundant in all wells.

Geophysical investigations undertaken in the Kamojang area have included resistivity, gravity, seismic (MEQ) and magnetic surveys. As well as independent 3D inversions of each dataset to resolve rock property contrasts, joint inversions have been undertaken using pairs of geophysical datasets, specifically seismic velocities (Vp and Vs) with gravity (density or porosity), and MT (resistivity) with gravity (density or porosity). An integrated interpretation of all the datasets, supported by petrophysical property measurements from a few drillhole cores, and reservoir measurements (temperatures and pressures), has helped inform the conceptual model for the physical setting of this vapour-dominated geothermal system (Figure 1).

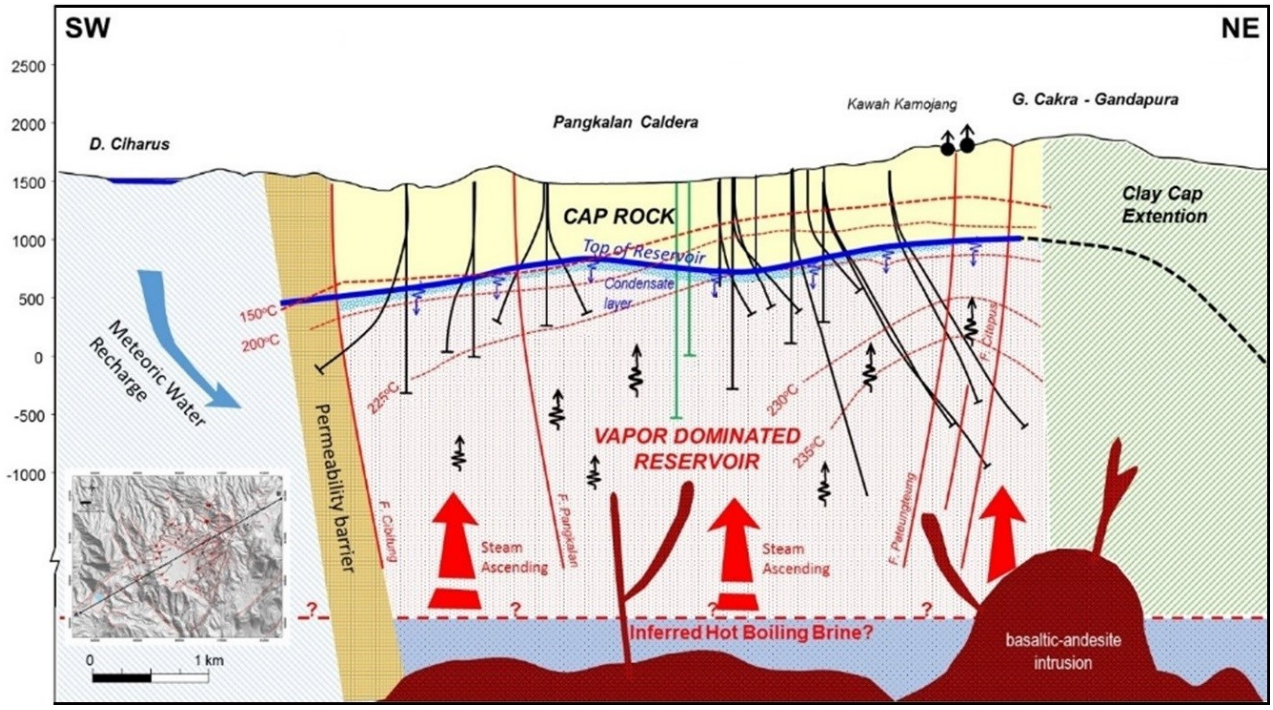

Figure 1: Cross-section showing the conceptual model of the Kamojang Geothermal Field (adapted from Prasetyo et al., 2020).

2.2 Leapfrog Digital Conceptual Model Update

Leapfrog digital conceptual models have become increasingly common tools for representing, analysing and interrogating geothermal conceptual models. Leapfrog allows users to visualise the conceptual model in 3D and enables better interaction between all the stakeholders in a geothermal development (O'Sullivan et al., 2019; Popineau et al., 2018). Leapfrog has the advantage that it can be used to tightly couple the digital conceptual model to numerical model through an integrated modelling framework that has been developed at the University of Auckland (O'Sullivan et al., 2019; Popineau et al., 2018).

However, before developing a numerical model coupled to the Leapfrog digital conceptual model, the Kamojang Leapfrog model needed to be updated to include latest conceptual model information and it needed to be revised so that it was consistent with our integrated modelling framework. Three main revisions were made:

- The geological model was extended laterally so that it covered the entire numerical model.
- The structural model was adapted, explicitly including more faults that can act as pathways or barriers for fluid flow.
- An inferred model of the shallow conductor (clay-cap) was included.

The lateral extent of the new Leapfrog model compared with the previous version is shown in Figure 2. The plots in Figure 3 show 3D views of geology, subsurface structures and alteration zone in the updated digital conceptual model.

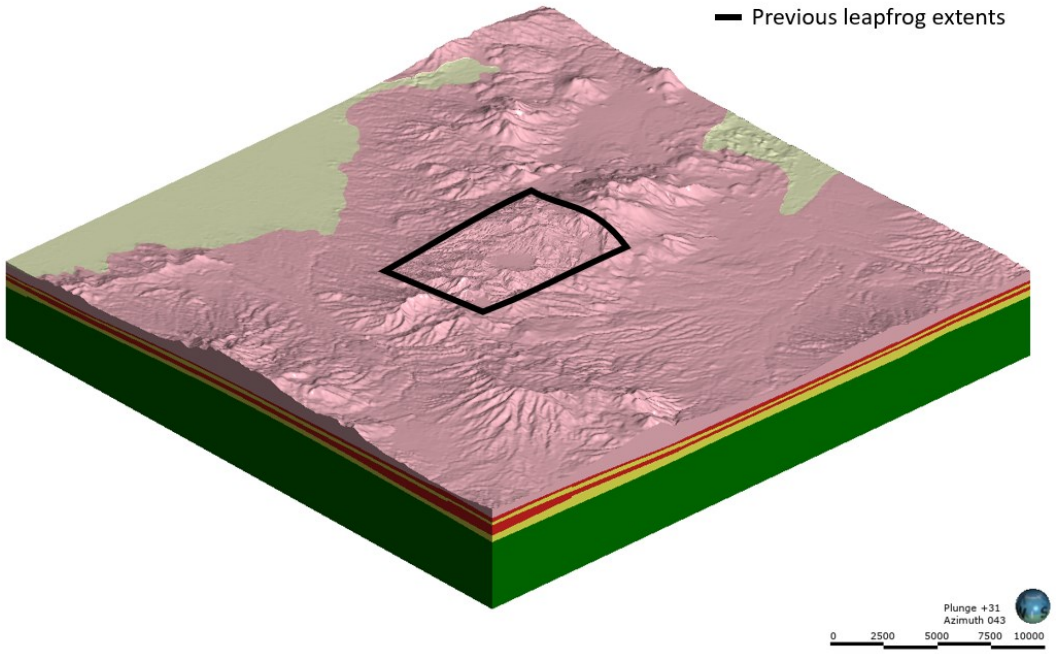

Figure 2: The new Leapfrog geological model of Kamojang. The extent of the previous model is shown in black.

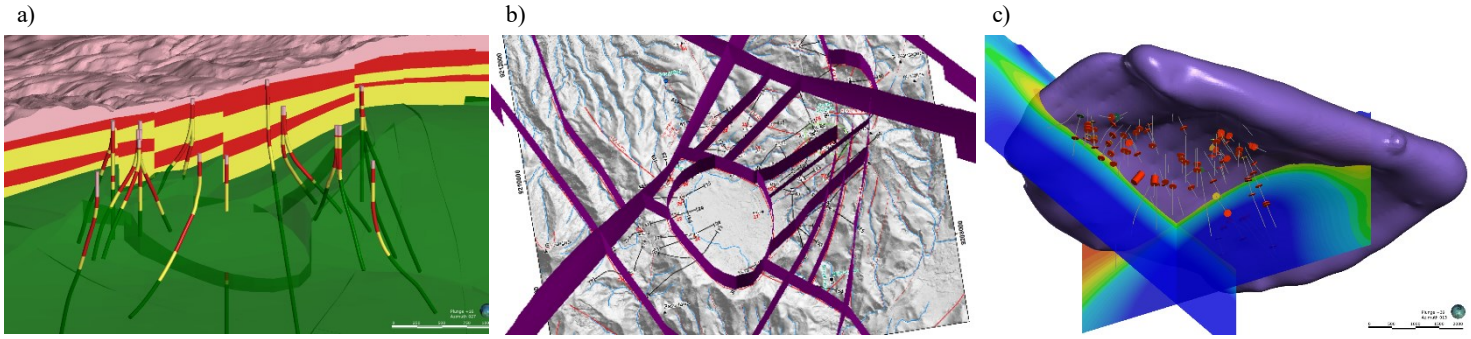

Figure 3: (a) A cut-away cross-section of the new Leapfrog geological model of Kamojang. (b) The new structural model shown above a map of the KGF. (c) The interpreted clay-cap viewed from below (purple) shown with MT resistivity slices and production wells with feedzones shown in red.

3. NUMERICAL MODEL REVIEW

An important stage in the project was to review the previous numerical models of the KGF and determine if the current model was appropriate for carrying out a resource assessment of the system. Our review is summarised below including discussion of the limitations of the existing model and our rationale to develop a new numerical model. The setup of the new numerical model, coupled to the Leapfrog digital conceptual model, is presented in the following section.

3.1 Previous numerical models

We had access to internal reports to review previous models developed by PGE, some with collaborators at Bandung Institute of Technology (ITB) (Institut Teknologi Bandung 2007, 2012; Pertamina Geothermal Energy, 2019, 2021). In addition, several open-source papers were consulted, including: O'Sullivan et al. 1990; Allis, 2000; Sasradipoera et al., 2000, Suryadarma et al. 2005; Suryadarma et al. 2010a; Yani et al. 2010.

The model set up by O'Sullivan et al, (1990) was relatively coarse with a total of 570 blocks (57 blocks per layer and 10 layers). It extended vertically from 1500 masl to -2000 masl. The 6 layers above sea level were 250 m thick and the 4 layers below sea level were 500 m thick. The area covered by the model was constrained within the DC resistivity boundary and recharge zone 2 km beyond the resistivity boundary. The size of the model was limited by the hardware and software available at that time. The simulator used was MULKOM, which was later modified to become TOUGH and then TOUGH2.

At the base of the model, hot-plate, i.e. constant Pressure, Temperature and gas saturation ($P/T/S_v$) boundary conditions were implemented and flow to the kawah (hot springs) was represented by a well on deliverability. The natural state model gave a good match to the measured reservoir pressures (and therefore also temperatures) and a flow to the kawah of 32.2 kg/s, close to the measured value of 35 kg/s (Hochstein, 1975). The calibration of the natural state model showed that the outer ring of recharge blocks had to have a very low permeability to prevent the vapour-dominated reservoir from being flooded.

A production history model was used to simulate 7 years of production at KGF and showed a reasonable match to the pressure declines in the wells KMJ-17 and KMJ-18. A future scenario was run and predicted that an output of 140 MW_e could be sustained for 30 years. Given the actual output of between 100 and 150 MW_e between 1990 and 2020, this has turned out to be a good prediction.

Allis (2000) did not specifically address modelling but did discuss mechanisms for the formation of vapour-dominated geothermal systems and was particularly helpful in guiding the setting up of our new numerical model.

Suryadarma et al. 2010a outline a collaborative modelling study by PGE and ITB. A numerical simulation was performed with natural state and production history matching followed by a 30-year future scenario simulation. The 3D numerical model contained 12,480 grid-blocks. It had a surface area of 49.5 km^2 and was divided into 15 layers covering a total depth of 3600 m. Reasonable results were shown for the natural state temperature profile in the well KMJ-14 and the pressure vs time decline for the well KMJ-27 from the production history simulation. The future scenario simulation predicted that increasing the electrical output capacity to 230 MW_e for the following 30 years (starting in 2009), by drilling 26–30 additional wells inside the 21 km^2 prospective area, could be possible.

The recent 2021 PGE model of Kamojang was implemented in TOUGH2 via the Petrasim interface. It consists of 3,456 model blocks, with 288 columns and 13 layers (including an atmospheric layer). The model extends vertically from 1500 masl to -2000 masl. Plot (a) in **Error! Reference source not found.** shows the lateral extent of the grid while plot (b) shows the vertical structure of the model. Overlaid in **Error! Reference source not found.**a is the proven zone (blue) as defined by PGE, the resistivity boundary (dashed blue) and the active structures included in the model. The structures included are the Kendang Fault, the Caldera, the Pateungteung Fault and the Citipus Fault.

From **Error! Reference source not found.** we can see that the 2021 PGE model is not large enough to capture the full (lateral and vertical) extent of the geothermal system. In general, we recommend that the model should extend 4-5 km laterally outside the hot reservoir and at least 1 km below the deepest well. Plot (a) in Figure 4 shows a large section within the resistivity boundary is not within the model domain which means that it cannot be included in forecast simulations.

Another problem with the 2021 PGE model is that the bottom boundary is set quite shallow (-2000 masl), i.e., 900 m below the inferred bottom of the reservoir (-1100 masl) and the constant $P/T/S_v$ boundary condition there may produce over-optimistic results for the future performance of Kamojang. The calibrated 2021 PGE natural state model gave a good match to most downhole temperature profiles and the production history model gave a reasonable match to the measured pressure declines.

a) b)

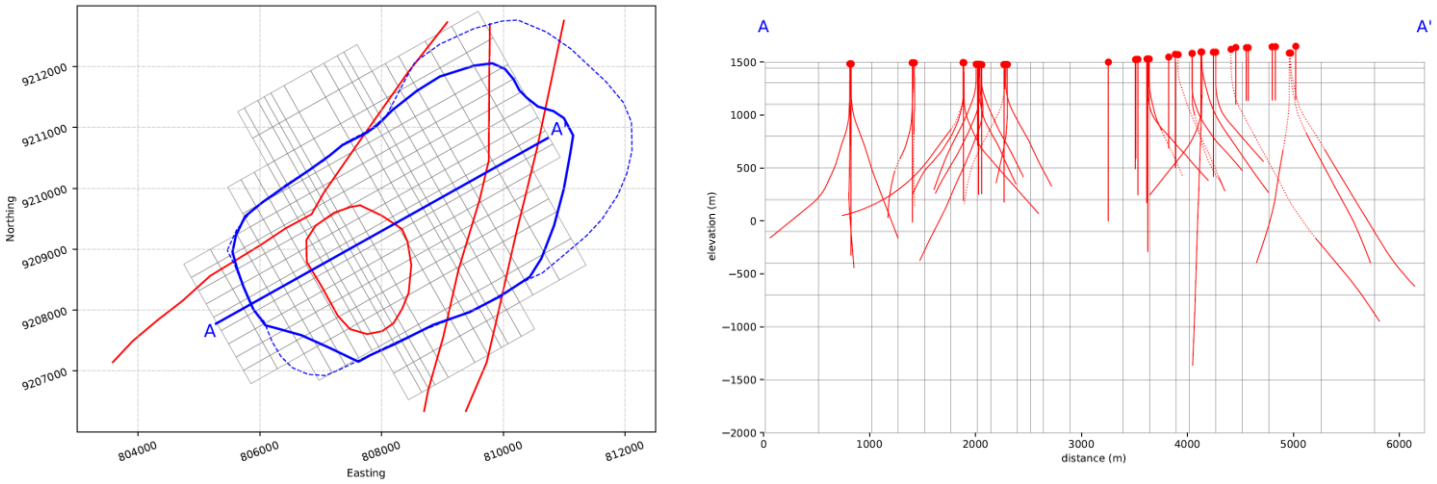

Figure 4: (a) Plan view of the previous PGE reservoir model grid. Proven resource shown in blue, resistivity boundary in dashed blue and structures included in the model are over laid in red. (b) Cross-section through the model showing the layer structure and a selection of production well tracks.

4. NUMERICAL MODEL DEVELOPMENT

Based on the limitations of the previous model as discussed above, a new numerical model was developed. In this section we outline the coupling of the new numerical model to the Leapfrog digital conceptual model and present the model setup.

4.1 Creation of the numerical model

In the workflow used in this project we coupled the Leapfrog digital conceptual model (including the geology, structural framework, and hydrothermal alteration) directly to a numerical model using our integrated modelling framework (O'Sullivan et al., 2019; Popineau et al., 2018). This means that the numerical model explicitly represents the best understanding of the geology and geophysical structure of the field. Faults, structures, and hydrothermal alteration are represented explicitly with rock-types which allow the properties of these features to be represented and provides heterogeneity to allow the model to be appropriately calibrated to reservoir engineering data. Figure 5 shows a comparison of the Leapfrog digital conceptual model and the coupled numerical model.

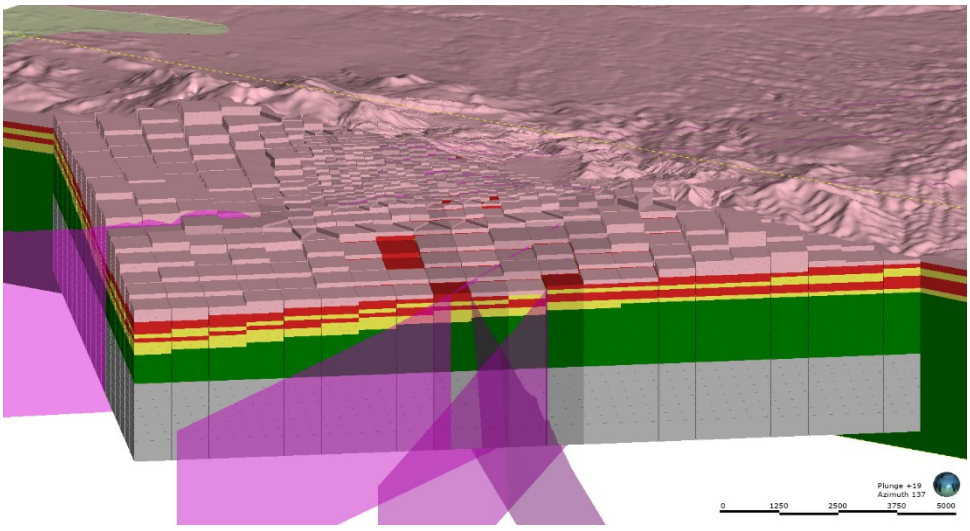

Figure 5: A comparison of the Leapfrog digital conceptual model on one side of the cross-section and the coupled numerical model on the other side. Magenta surfaces indicate structures in the digital conceptual model with the corresponding numerical model blocks shaded.

4.2 Model grid

The grid selected for the new numerical model is shown in Figure with well tracks superimposed and the resistivity boundary included. A SW-NE vertical slice through the model is shown in Figure . There were several criteria which determined the design of the new grid:

- The smallest blocks are small enough (200 m x 200 m) to provide reasonable resolution.
- A large area around the hot reservoir is included to allow cold recharge to be represented in the model.
- The fine grid extends far enough to the NE to include the full resistivity boundary.
- The top of the model is at ground surface and thus follows the topography (see Figure). Thus, the model includes the shallow unsaturated zone.
- The base of the model is set at -3000 masl. This is 1900 m below the base of the reservoir at -1100 masl.

The new model has 48,003 blocks, with 1,312 columns and 54 layers.

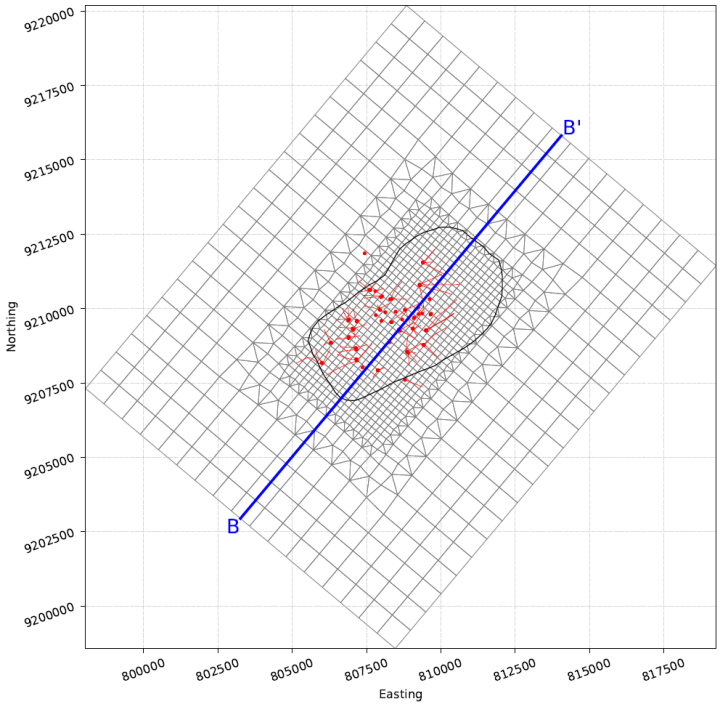

Figure 6: Plan view of the model grid showing the resistivity boundary (black) and the well tracks (red). B-B' defines a cross-section used in subsequent figures.

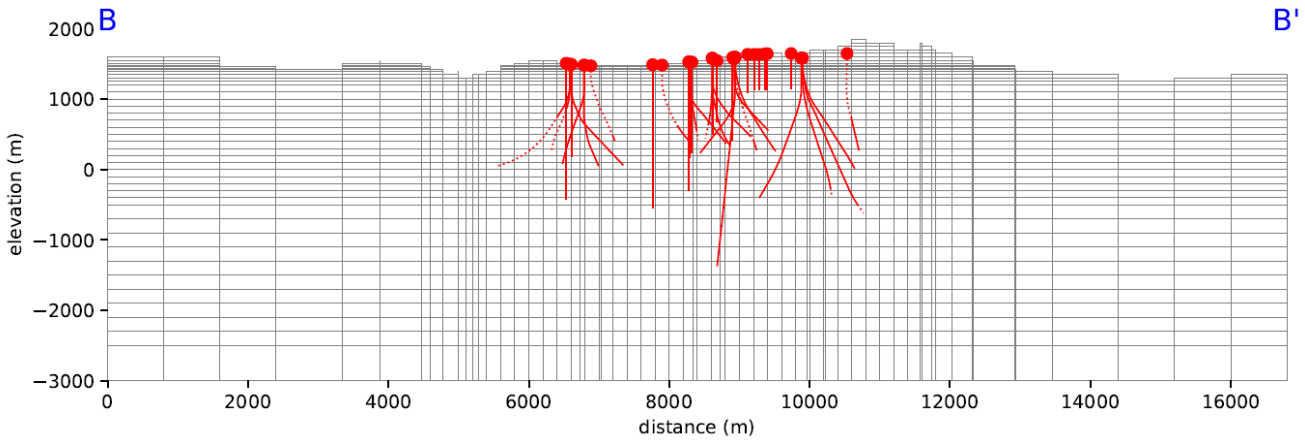

Figure 7: SW-NE vertical slice (B-B' as defined in Figure) through the model grid showing well tracks and topography

4.3 Boundary conditions

In this section we discuss the boundary conditions used in the new model.

Top boundary

Constant temperature of 24 °C and atmospheric pressure are set at the top of the model. In addition, rainfall at 24 °C (enthalpy of 100.7 kJ/kg) is injected in the top of the model at a rate of 5.9 x 10^{-7} kg/s m^2. This corresponds to an annual rainfall of 2960 mm/year and an infiltration rate of 10%.

Side boundary

All sides are treated as no-flow boundaries for both heat and mass. This is a reasonable assumption as the boundaries are well away from the edges of the reservoir.

Bottom boundary

Vapour-dominated geothermal systems require hot-plate boundary conditions (constant pressure, temperature and vapour saturation) at the base of the model (McGuinness and Pruess, 1987; McGuinness et al., 1993) instead of the heat and mass flow boundary conditions used in models of other types of geothermal systems. Constant temperature and constant vapour saturation boundary conditions (340 °C and 0.5, corresponding to a pressure of 146.05 bar) are set at the base of the model below the reservoir. These boundary conditions are implemented with very large volume blocks (layer 54) over part of the model (see Figure). On the rest of the model a background heat flux of 80 mW/m^2 is specified (in layer 53).

The extent of the hot-plate, applied only over part of the model as shown in Figure 8, could be described as conservative. The upflow conceptually extends further NE beyond the proven part of reservoir (where some future make-up wells are targeted).

Springs

The hot springs are implemented by wells-on-deliverability located in layer 29 (centered at 850 masl) near the top of the reservoir.

4.4 Geothermal simulators

The new numerical model is set up to be run in either AUTOUGH2 (Yeh et al., 2012), a local variant of the industry-standard simulator TOUGH2 (Pruess et al., 1985), or in Waiwera (Croucher et al., 2016, 2017, 2018, 2020; O'Sullivan et al., 2017, Burnell et al., 2015), a highly parallelised, open-source simulator developed by the University of Auckland and GNS Science. Running the model interchangeably using both simulators leverages the power of Waiwera for fast calibration times and rapid model development while retaining the confidence that TOUGH2 provides as the industry-standard simulator.

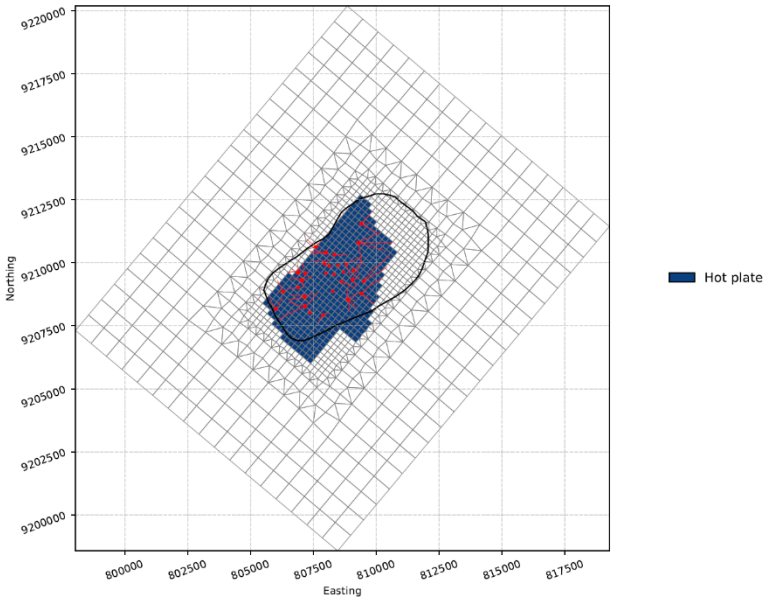

Figure 8: Constant P/T/Sv hot-plate at the base of the model (layer 54). The resistivity boundary is shown in black and the well tracks in red.

5. NUMERICAL MODEL CALIBRATION

5.1 Natural state calibration

The large-scale objectives of natural state calibration were as follows:

- To achieve a temperature at the bottom of the reservoir of ~ 250 °C
- To have a mass flow from the three springs of 35 kg/s
- To have vapour saturations in the reservoir close to the immobile liquid value (taken as 0.5 in the model).

To achieve these aims the following quantities were found to be the most influential parameters:

- Base temperature
- Average vertical permeability in the low permeability basement (-1100 masl to -3000 masl)
- Average vertical permeability in the reservoir (above -1100 masl)

As mentioned above in Section 4 the base temperature was set to 340 °C. The vertical permeability distribution for the calibrated model is shown in Figure . The calibrated model permeabilities give the following insights into the permeability structure of the KGF:

- Outside the reservoir vertical permeabilities are very low (dark blue in Figure): 1.3E-16 m^2
- Background permeabilities are low beneath the reservoir (light green in Figure): 1.1E-15 m^2
- Several faults are likely to have high vertical permeability in basement (orange in Figure): 3.68E-15 m^2
- Other faults are likely to have medium vertical permeability in basement (yellow in Figure): 2.50E-15 m^2

In general, the match of the calibrated natural state model results to the measured data is good. There are mismatches in some wells but there is also some uncertainty in the temperature data since downhole temperature measurements were made long after production started at the KGF and there is evidence of temperature evolution over time. Examples of the downhole temperature plots from the calibrated model against measured data are shown in **Error! Reference source not found.**.

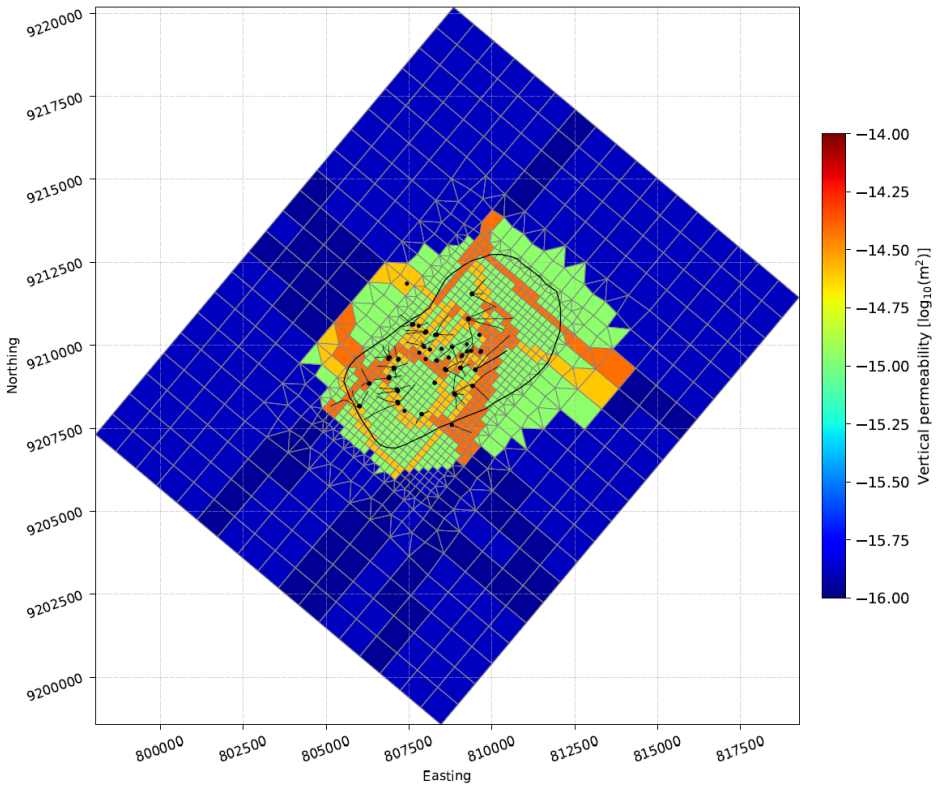

Figure 9: Vertical permeability in the basement of the calibrated model.

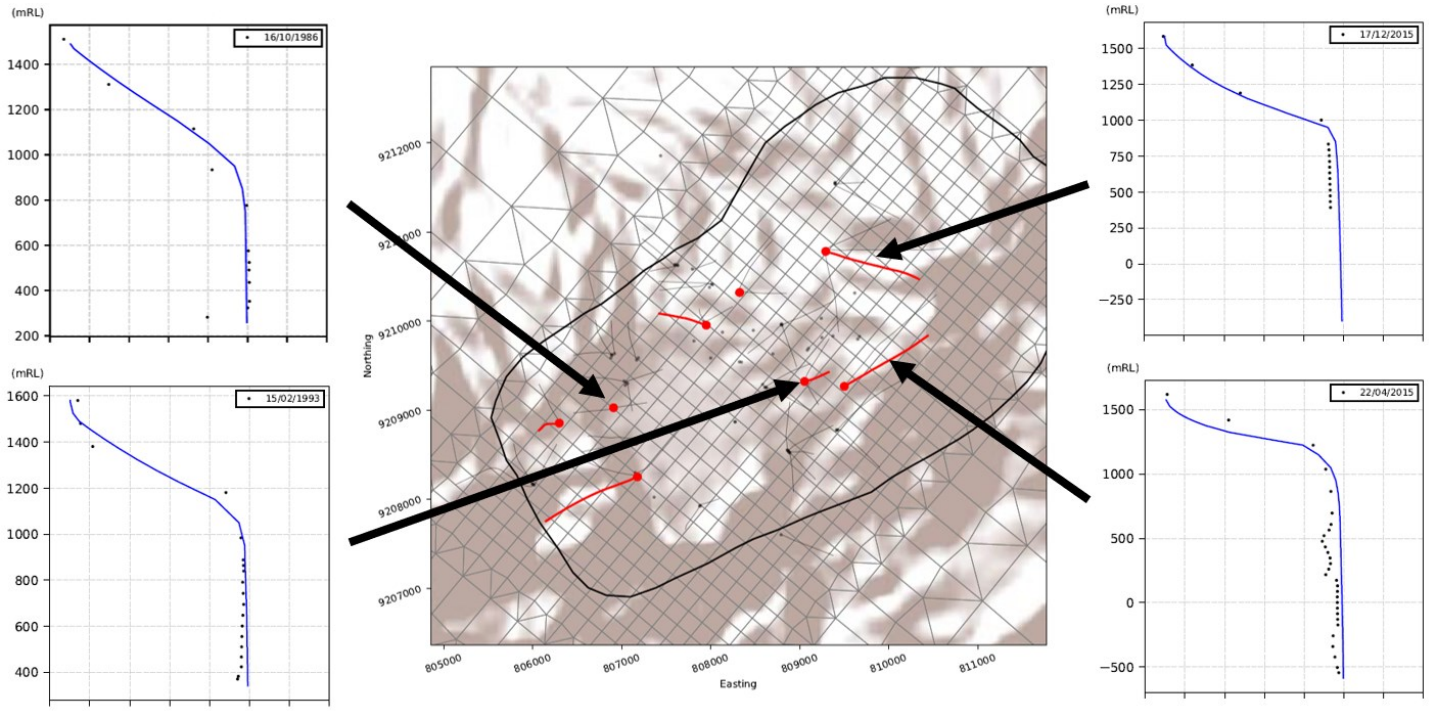

Figure 10: Downhole temperature vs elevation for selected wells including their location in the KGF. Model results are given in blue and measured data in black.

Temperatures on a vertical slice through the calibrated model (defined in Figure 6) are shown in Figure . The corresponding vapour (or gas) saturation is shown in Figure . It shows some "wetting" of the sides of the basement below the reservoir and possibly even lower lateral permeability should be used in the outer area of the basement (dark blue in Figure) though there is some evidence of a liquid level encountered at depth in some of the deepest production wells.

The small unsaturated zone (vadose zone) at the top of the model is shown in Figure .

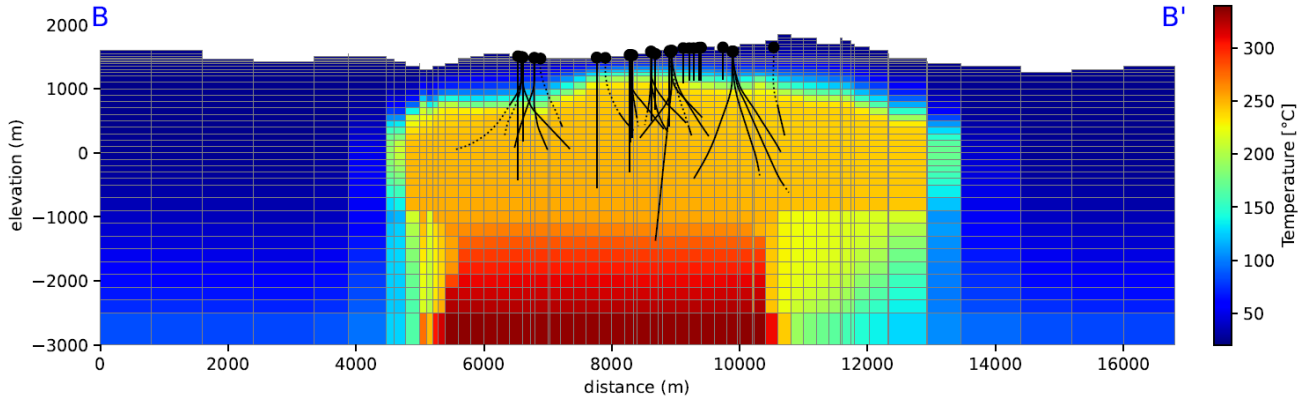

Figure 11: Natural state model temperatures on a SW-NE vertical slice (along B-B' as defined in Figure).

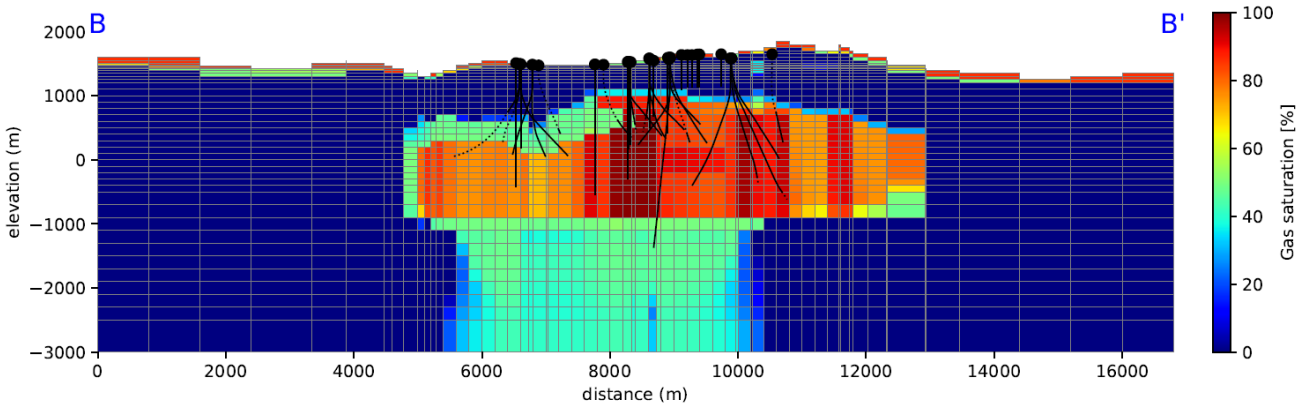

Figure 12: Natural state model vapour saturations on a SW-NE vertical slice (along B-B' as defined in Figure).

5.2 Production history calibration

The production history model was calibrated by adjusting local permeability and porosities to match measured transient pressure data. For the production history a dual porosity model was used. In a dual porosity model, high-permeability, low-volume fractures are embedded in a low permeability matrix. In TOUGH2 this dual continuum is represented by the MINC system (Pruess and Narasimhan, 1985) with each block of the single porosity model partitioned into a fracture block and one or more matrix blocks. The parameters used are shown in Table .

Table 1: Dual porosity parameters used in the production history model

Parameter	Value
Number of matrix blocks	2 (20% and 75%)
Volume fraction of fracture blocks	5%
Fracture spacing	25 m
Fracture planes	3
Permeability of matrix	1.0E-16 m^2
Porosity of matrix	6.3%, 16.8% or 22.1%
Permeability of fractures	variable
Porosity of fractures	variable

Overall, a very good match was achieved between the production history model and measured transient pressure data. A typical page of plots is shown in Figure 13 where the match to the data for the pressure decline and the enthalpy response for the well is very good. A similar high quality of match to the data for pressure decline and enthalpy response is achieved for most wells.

For a few production wells the interference from nearby injection is overestimated by the model with the enthalpy dropping below that of dry steam. This aspect of model performance could be improved with more time spent on calibration, or possibly some mesh refinement will be required to obtain better separation of production and injection wells. However, this problem with the model is conservative in the sense that it will result in an underestimate of future steam flows and hence MW_e output.

One of the features of the development of vapour-dominated geothermal systems such as KGF is that they tend to dry-out, i.e., they run out of immobile water before they run out of heat. From measured data, PGE have deduced that several wells have become superheated. They have calculated a degree of superheat for these wells, and it has been used as an additional calibration tool for the numerical model. The measured data is not a complete data set and the model calibration is not a perfect match but the results show that the calibrated model also achieves a good qualitative match to the evolution of the superheated zones in the reservoir.

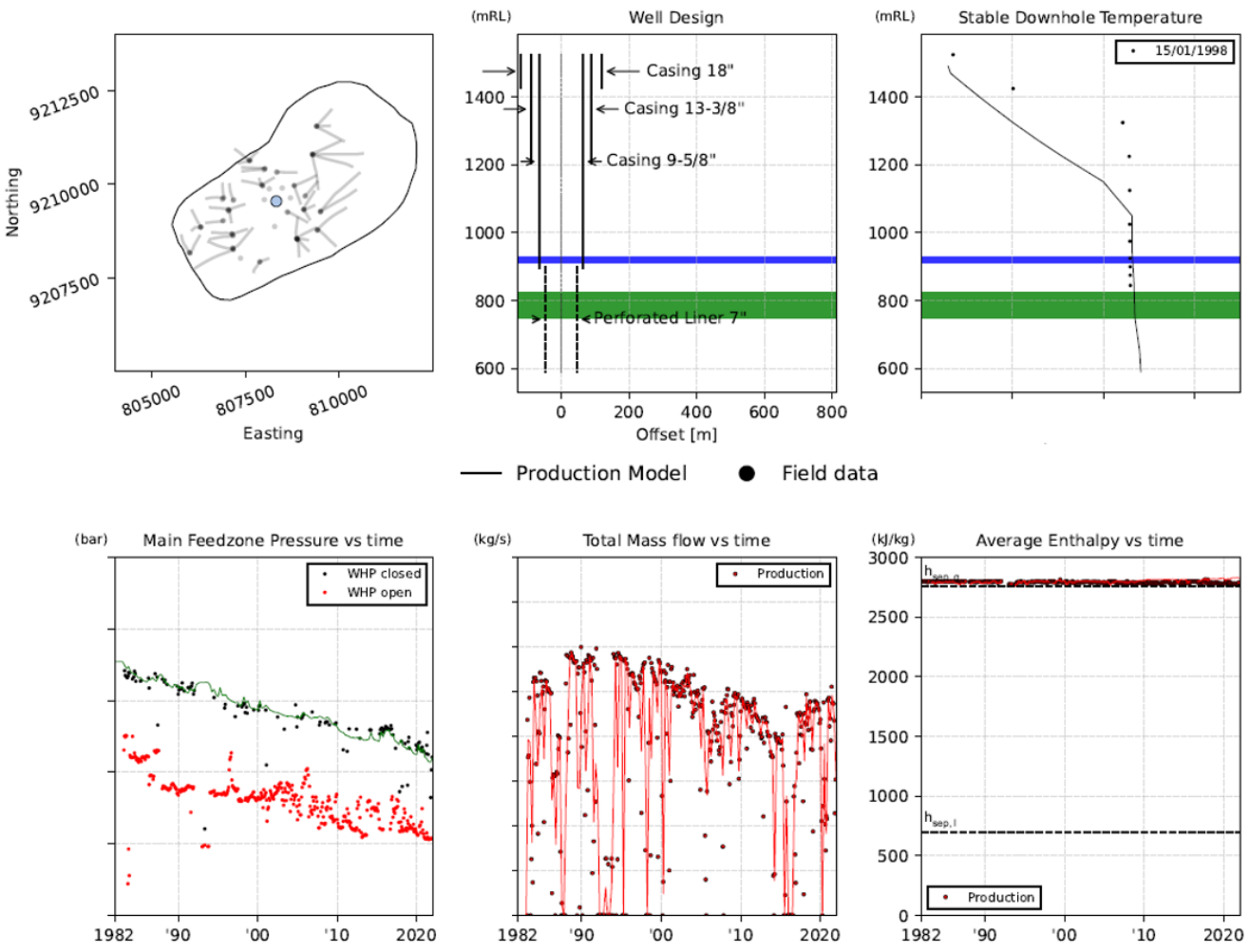

Figure 13: Typical calibrated production history model results for a production well. Model results shown as solid lines and measured data as symbols.

5. MODEL FORECASTS

The calibrated production history model has been used to make a range of forecasts about the future behaviour of the KGF. Scenarios investigated so far include:

- Targeting future make-up wells
- Scheduling make-up wells
- Assessing the resource potential through various make-up well scenarios
- Testing reinjection strategies

The future scenarios are all run using the same dual porosity model set up as the production history model. However, existing production wells and future make-up wells are represented by wells on deliverability with properties determined using detailed wellbore modelling. Model results from the future scenarios are visualised through standardised sets of reports but can also be easily loaded into Leapfrog to generate 3D views and animations to help understand and communicate the findings of the modelling studies.

Numerical modelling of geothermal systems is affected by many types of uncertainty. These include, but are not limited to, uncertainty in the measured data, uncertainty in the unknown structure of the subsurface, uncertainty in the future operation of the resource and uncertainty in the model parameters.

The numerical modelling project of the KGF includes all these uncertainties and quantifying the level of uncertainty in the forecasts from the new model was outside the scope of this project. However, well-established geothermal modelling practices were used to develop the new model, and therefore it is likely to produce accurate forecasts.

6. CONCLUSIONS

This paper discusses a new modelling study of the Kamojang Geothermal Field carried out by a multidisciplinary team made up of members from PT. Pertamina Geothermal Energy, the Geothermal Institute at the University of Auckland, Geoenergis Solusi Indonesia, and independent New Zealand geothermal experts. The project successfully achieved its objectives through close collaboration and an inclusive, transparent approach.

A review and update of the conceptual model of Kamojang were conducted resulting in an updated digital conceptual model, implemented in the Leapfrog Geothermal software. The new Leapfrog model was developed using well-established conceptual modelling techniques and is consistent with the data provided. It covers a larger area and has a more detailed representation of the geothermal system than the existing Leapfrog model used by PGE.

Limitations in the existing numerical model required a new numerical model to be set up. The new numerical model was created following well-established numerical modelling techniques that ensure the model is consistent with the conceptual model and capable of accurately representing the behaviour of the Kamojang Geothermal Field over time.

The key differences between this new numerical model of Kamojang and the existing PGE model are:

- It covers a much larger area than the PGE numerical model and includes both the full area covered by the resistivity boundary of the resource in the NE and peripheral recharge zones.
- It extends vertically up to the ground surface, thus following the topography and including the unsaturated zone in the model allowing for a better representation of shallow pressures.
- It extends down to a base at -3000 masl, 1900 m below the base of the reservoir providing better representation of the deep reservoir conditions.
- It is tightly coupled to the geological and geophysical data in the digital conceptual model ensuring consistency.
- It is a dual-porosity model explicitly modelling flow in fracture pathways enabling a more accurate representation of pressure and enthalpy changes over time.

The new numerical model was calibrated against the measured data provided by PGE using the industry-standard approach. The natural state model was calibrated against all the available downhole temperature profiles and then the production history model was calibrated against the available pressure decline and enthalpy response data. A satisfactory match to the temperature profiles and a very good match to the pressure decline and enthalpy response data were obtained.

The state of model calibration achieved is good and therefore, we are confident that the model provides a good representation of the Kamojang Geothermal Field and is appropriate to use for forecasting.

7. ACKNOWLEDGEMENTS

The authors would like to thank PT. Pertamina Geothermal Energy for permission to publish this work.

REFERENCES

Allis R. 2000. Insights on the formation of vapour dominated geothermal systems.. *Proc. World Geothermal Congress 2000*, Japan, May28-June10, p2490-2496.

Browne, P.R.L., 1977. Petrologic Report: Kawah Kamojang Drillhole KK12. Dept. of Scientific & Industrial Research, New Zealand Geological Survey.

Burnell, J., O'Sullivan, M., O'Sullivan, J., Kissling, W., Croucher, A., Pogacnik, J., Pearson, S., Caldwell, G., Ellis, S., Zarrouk, S. and Climo, M.: Geothermal Supermodels: the Next Generation of Integrated Geophysical, Chemical and Flow Simulation Modelling Tools. *Proc. World Geothermal Congress 2015*, Melbourne, Australia, 19-25 April (2015).

Croucher, A., O'Sullivan, M. J., O'Sullivan, J. P., Pogacnik, J., Yeh, A., Burnell, J., Kissling, W., 2016. Geothermal supermodels project: An update on flow simulator development. Proc. 38th New Zealand Geothermal Workshop. Auckland, New Zealand.

Croucher, A. E., O'Sullivan, M. J., O'Sullivan, J. P., Pogacnik, J., Yeh, A., Burnell, J., Kissling, W., 2017. Geothermal Supermodels project: an update on flow simulator development. Proc. 39th New Zealand Geothermal Workshop. Rotorua, New Zealand.

Croucher, A. E., O'Sullivan, J. P., Yeh, A., O'Sullivan, M. J., 2018. Benchmarking and experiments with Waiwera, a new geothermal simulator. Proc. 43rd Workshop on Geothermal Reservoir Engineering. Stanford University, Stanford, California, USA.

Croucher, A., O'Sullivan, M.J., O'Sullivan, J.P., Yeh, A., Burnell, J., Kissling, W., 2020. Waiwera: a parallel open-source geothermal flow simulator. Computers and Geosciences 141. https://doi.org/10.1016/j.cageo.2020.104529

Healy, J., 1977. Kawah Kamojang Geothermal Field. Geological Progress Report for Dept. of Scientific & Industrial Research, New Zealand Geological Survey

Hochstein, M.P., 1975. Geophysical exploration of the Kawah Kamojang geothermal field, West Java, Proc. Second UN Symposium on the Development and Use of Geothermal Resources, 1049-1058.

McGuinness, M.J., Pruess, K., 1987, Unstable heat pipes. Proc. 9th New Zealand Geothermal Workshop, Auckland, New Zealand, 47-51.

McGuinness, M.J., Blakeley, M., Pruess, K., O'Sullivan, M.J. (1993). Geothermal heat pipe stability: Solution selection by upstreaming and boundary conditions. *Transport in Porous Media*, *11*(1), 71-100. Doi:10.1007/bf00614636

O'Sullivan, M.J., Barnett, B.G., Razali, M., Y., 1990, Numerical Simulation of the Kamojang Geothermal Field, Indonesia. *Transactions Geothermal Resources Council v14, Part 2. p1317-1324.*

O'Sullivan, J.P., Croucher, A.E., Yeh, A., O'Sullivan, M.J., 2017. Experiments with Waiwera, a new geothermal simulator. Proc. 39th NZ Geothermal Workshop, Rotorua, New Zealand.

O'Sullivan, J. P., Croucher, A.E, Popineau, J., Yeh, A., O'Sullivan, M.J., 2019. Working with multi-million block geothermal reservoir models. Proc. 44th Workshop on Geothermal Reservoir Engineering, Stanford University, Stanford, California, USA.

Popineau, J., O'Sullivan, J.P., O'Sullivan, M.J., Archer, R., Williams, B., 2018. An integrated Leapfrog/TOUGH2 workflow for a geothermal production modelling. Proc. 7th African Rift Geothermal Conference (ARGeo). Kigali, Rwanda.

Prasetyo, I.M., Sardiyanto, Larasati, D., Yuniar, D., Hastuti, P., Adi, T., 2020. Kamojang Geothermal Field Conceptual Model Update, Internal Report, Dec. 2020, PT. Pertamina Geothermal Energy.

Pruess, K., Narasimhan, T.N. (1985) A Practical Method for Modeling Fluid and Heat Flow in Fractured Porous Media, *Society of Petroleum Engineers Journal,* 25(1), 14-26.

Sasradipoera, D.S., Sujata, I.K., Komaruddin, U., 2000. Evaluation of steam production decline trends in the Kamojang geothermal field. Proceedings World Geothermal Congress 2000, Kyushu-Tohuku, Japan, May 28 – June 10, 2000.

Suryadarma, Azimuddin, T., Dwikorianto, T., Fauzio, A., 2005. The Kamojang Geothermal Field: 25 Years Operation. Proceedings World Geothermal Congress 2005, Antalya, Turkey, 24-29 April 2005.

Suryadarma, Dwikorianto, T., Zuhro, A. A., Yani, A., 2010a. Sustainable development of the Kamojang geothermal field, Geothermics 39 (2010) 391–399.

Suryadarma, Dwikorianto, T., Zuhro, A. A., 2010b. Lessons Learned from Kamojang Geothermal Steam Field Management: from the Beginning Until Now. Proceedings World Geothermal Congress 2010, Bali, Indonesia, 25-29 April 2010.

Wood, C.P., 1975. Petrological Report: Cores from Kawah Kamojang 10. Dept. of Scientific & Industrial Research, New Zealand Geological Survey.

Yani A., 2010. Steam Ratio Obtained From the Mass Amount of Condensate Reinjection by Means of Monitoring the Performance of Groups of Production Wells 140 MWe Geothermal Field Kamojang – Indonesia. *Proceedings World Geothermal Congress 2015* Melbourne, Australia, 19-25 April 2015.

Yeh, A., Croucher, A. E., O'Sullivan, M.J., 2012. Recent developments in the AUTOUGH2 simulator. Proc. TOUGH Symposium 2012. Lawrence Berkeley National Laboratory Berkeley, California, USA.